Supplementary Information

Engineering the linkage of mesoporous covalent organic frameworks for enhancing photocatalytic selective oxidation of organic sulfides

Jiaqi Zhang, Yuexin Wang, Zheng Li, Siyu Zhang and Xianjun Lang*

Hubei Key Lab on Organic and Polymeric Optoelectronic Materials, College of Chemistry and Molecular Sciences, Wuhan University, Wuhan 430072, China.

**To whom correspondence should be addressed. E-mail address: xianjunlang@whu.edu.cn.*

1 Materials and methods

1.1. Reagents and solvents

TFPT and TDA were purchased from Adamas and TCN was purchased from Innochem. Other reagents, including the organic sulfide substrates and solvents, were purchased from Sigma-Aldrich, TCI, Innochem, Adamas, Alfa Aesar, Sinopharm Chemical Reagent, etc. All commercially available reagents and solvents were used without further purification.

1.2. Characterizations

The crystal phase composition of solid samples was identified by powder X-ray diffraction (PXRD) using a Rigaku Miniflex 600 and SmartLab SE diffractometer with a filtered Cu K_α line, and the patterns were gathered from 1.5° to 30° at room temperature. The Fourier transform infrared (FTIR) spectra were recorded out by Nicolet 5700 FTIR Spectrometer with Continuum IR Microscope ranging from 400–4000 cm^{-1}. Solid-state ^{13}C NMR spectra were performed on 400 MHz spectrometers (AVANCE NEO 400). X-ray photoelectron spectroscopy (XPS) data were collected using an ESCALAB 250Xi spectrometer (Thermo Fisher Scientific). Field-emission scanning electron microscopy (FE-SEM) images of organic materials were measured on Zeiss Merlin Compact field emission scanning electron microscope. The high-resolution transmission electron microscopy (HRTEM) images and energy dispersive spectroscopy (EDS) elemental mapping were estimated on a JEM-F200. The N_2 isotherms and specific surface areas were determined at 77 K employing a

Micromeritics ASAP 2460 automated system with the Brunauer–Emmet–Teller (BET) model, and the pore size and volume were derived from the sorption curve by using non-local density functional theory model, the materials were degassed in vacuum (< 1×10^{-5} bar) at 120 °C for 12 h. The UV–visible absorption spectra were detailed on a Shimadzu UV−3600 UV−visible spectrophotometer with a diffuse reflectance measurement accessory. Photoluminescence (PL) and Time-resolved PL (TRPL) spectrum was obtained with an Edinburgh FS5 spectrophotometer. The electron paramagnetic resonance (EPR) spectra were collected on a JEOL, JES−FA300 EPR spectrometer.

1.3. Electrochemical measurements

Electrochemical measurements were executed on a Metrohm Autolab PGSTAT302N in a three-electrode electrochemical cell equipped with an electrochemical station. Firstly, 2 mg of photocatalyst was dispersed in 1 mL of 0.2 wt% Nafion by 5 min ultrasonification. Then, the samples were dripped on ITO-coated glasses which were placed on top of a glassy carbon served as the working electrode, and the samples were dried under infrared irradiation. With 0.1 M Na_2SO_4 aqueous solution supplied as the electrolyte, the Ag/AgCl electrode and platinum wire were the reference electrode and counter electrode, respectively. Meanwhile, the 460 ± 10 nm blue LEDs (Shenzhen Ouying Lighting Science and Technology Co., Ltd.) placed 2 cm away from the photoelectrochemical cell were employed as the light source.

1.4. The typical operation for the selective oxidation of sulfides

COF (5 mg), methanol (MeOH) (1 mL), and sulfide (0.3 mmol) were subsequently added into a Pyrex photoreactor (10 mL), which was stirred under darkness for 10 min to achieve adsorption–desorption equilibrium. After that, the reactor was irradiated directly by 460 nm blue LEDs (3 W × 4) and kept stirring at 1500 rpm under 0.1 MPa O_2. After releasing the excess O_2, the supernatant from the centrifuged mixture was detected through gas chromatography−mass spectrometry (GC−MS) and further precisely quantified by gas chromatography−flame ionization detection (GC−FID).

Conversion of organic sulfide and selectivity of organic sulfoxide were calculated as follows:

$$\text{Conversion (\%)} = [(C_0 - C_S) / C_0] \times 100$$

$$\text{Selectivity (\%)} = [C_p / (C_0 - C_S)] \times 100$$

where C_0 is the initial concentration of sulfide substrate; C_S and C_p are the concentrations of organic sulfide and sulfoxide product at a certain time during the photocatalytic reaction.

1.5. Density functional theory (DFT) calculations

DFT calculations were carried out using the Gaussian 16W program package. Gaussian View 6.0 was used for the visualization. In short, the simplified unit consisting of COFs was taken into consideration. Molecular geometries were optimized using B3LYP/6-31G (d). In addition, the Gibbs free energies for the adsorption of thioanisole and methyl phenyl sulfoxide on both COFs were also calculated.

2. Results

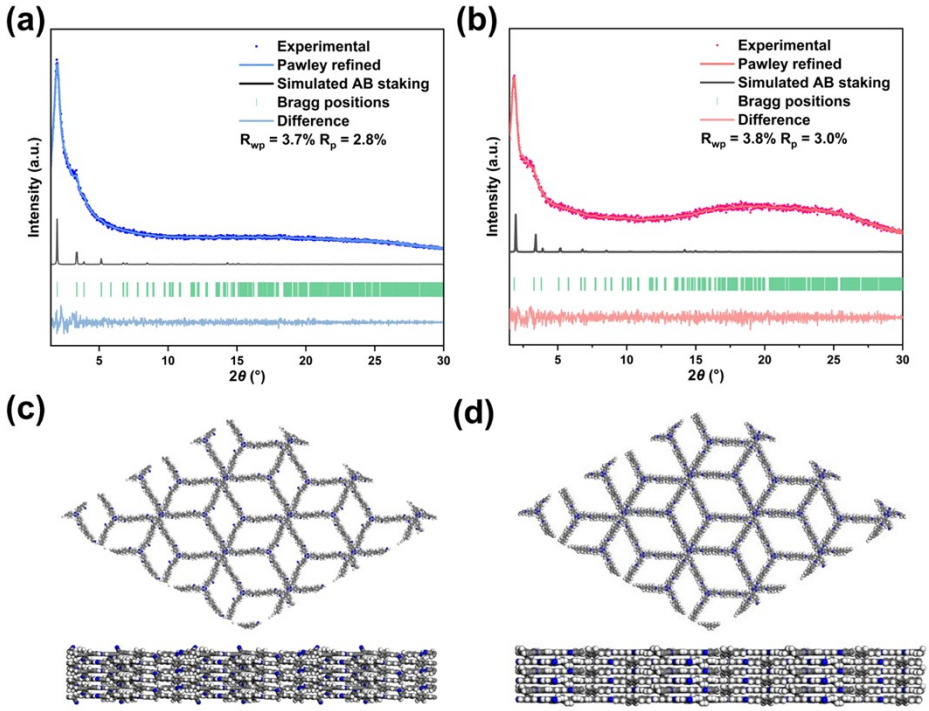

Fig. S1. Experimental, Pawley refined, and simulated PXRD patterns of TFPT-sp^{2}c-TCN (a) and TFPT-TDA (b). The top and side views of the eclipsed AB stackings of TFPT-sp^{2}c-TCN (c) and TFPT-TDA (d). Pawley refinement yielded unit lattice parameters of a = 52.5 Å, b = 52.0 Å, c = 6.2 Å, and $\alpha = \beta$ = 90.0°, γ = 120.0°, with R_{wp} = 3.7% and R_p = 2.8% for TFPT-sp^{2}c-TCN; a = 52.3 Å, b = 52.0 Å, c = 6.3 Å, and $\alpha = \beta$ = 90.0°, γ = 120.0°, with R_{wp} = 3.8% and R_p = 3.0% for TFPT-TDA.

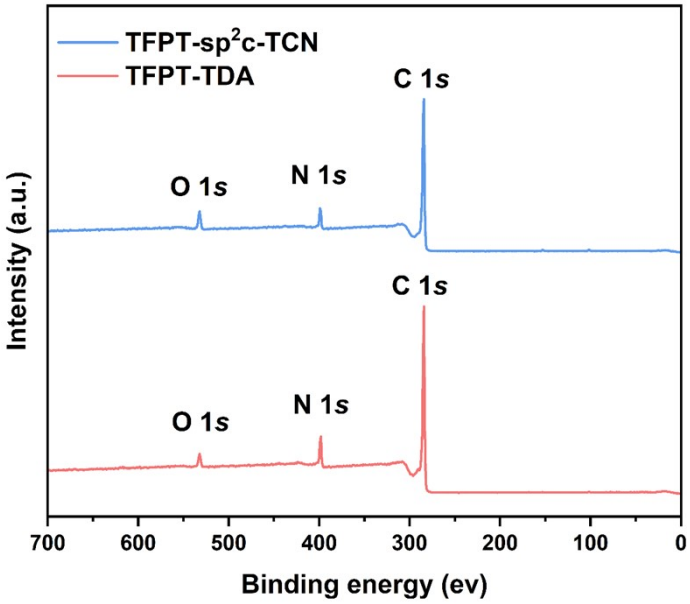

Fig. S2. XPS survey spectra of TFPT-sp^{2}c-TCN and TFPT-TDA.

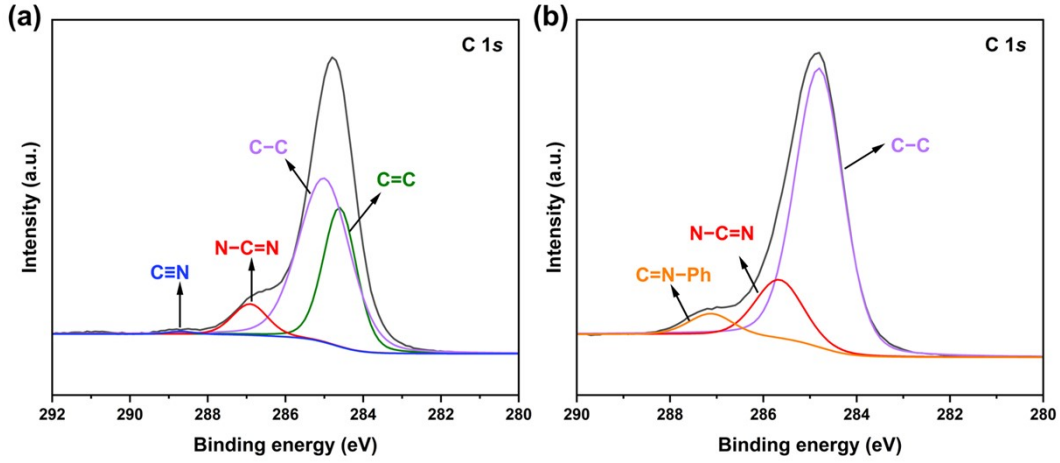

Fig. S3. C 1*s* XPS spectra of TFPT-sp^{2}c-TCN and TFPT-TDA.

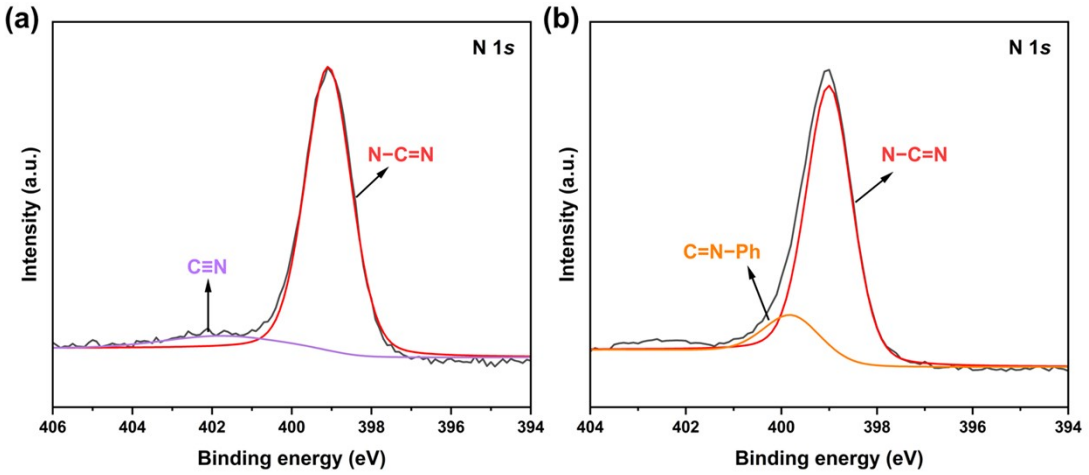

Fig. S4. N 1*s* XPS spectra of TFPT-sp^{2}c-TCN and TFPT-TDA.

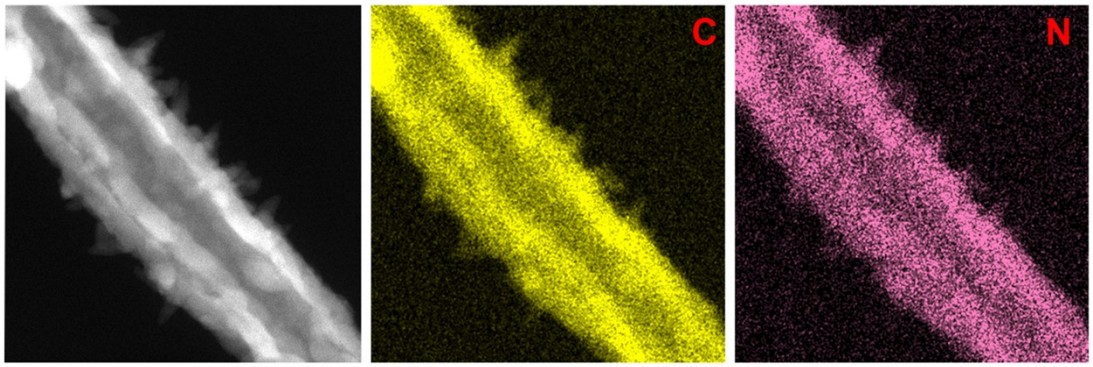

Fig. S5. The TEM image of the TFPT-sp^{2}c-TCN and the corresponding EDS mapping of C, N.

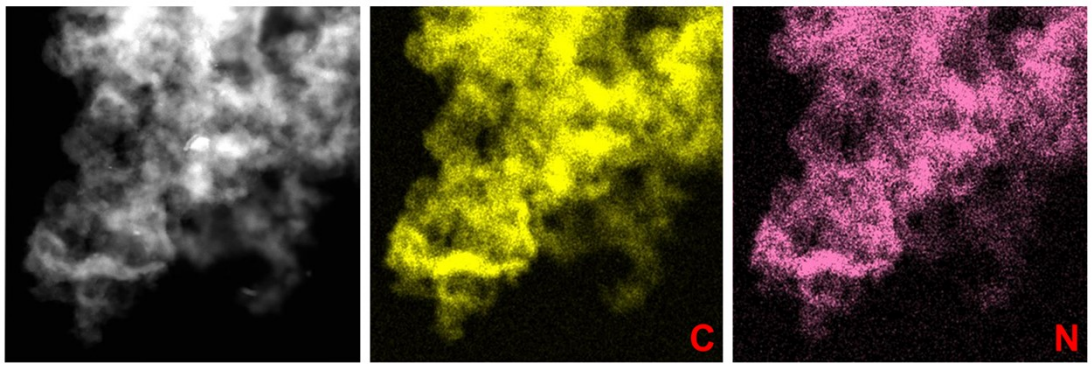

Fig. S6. The TEM image of the TFPT-TDA and the corresponding EDS mapping of C, N.

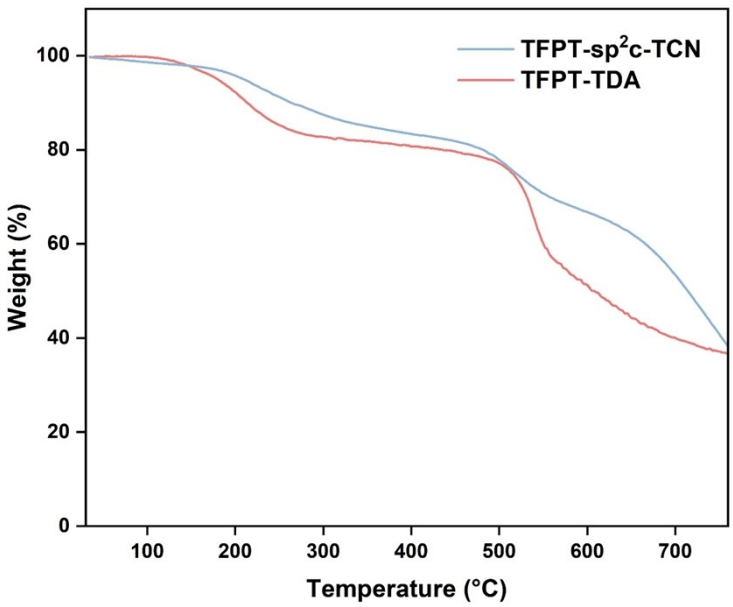

Fig. S7. TGA curves of TFPT-sp^{2}c-TCN and TFPT-TDA.

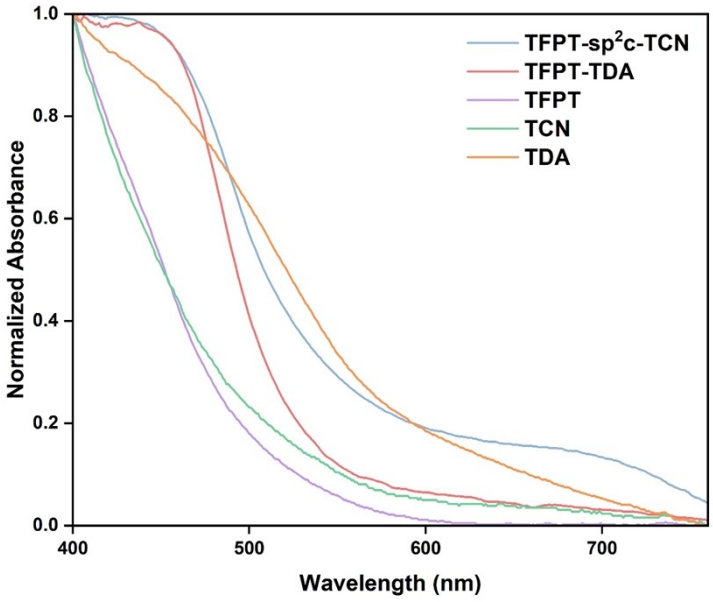

Fig. S8. UV–vis DRS spectra of TFPT-sp^{2}c-TCN, TFPT-TDA, TFPT, TCN and TDA.

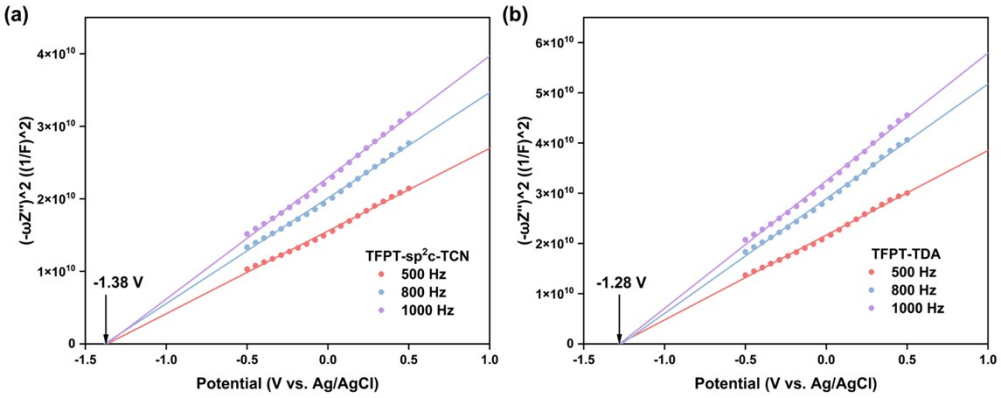

Fig. S9. Mott–Schottky plots of TFPT-sp^{2}c-TCN (a) and TFPT-TDA (b).

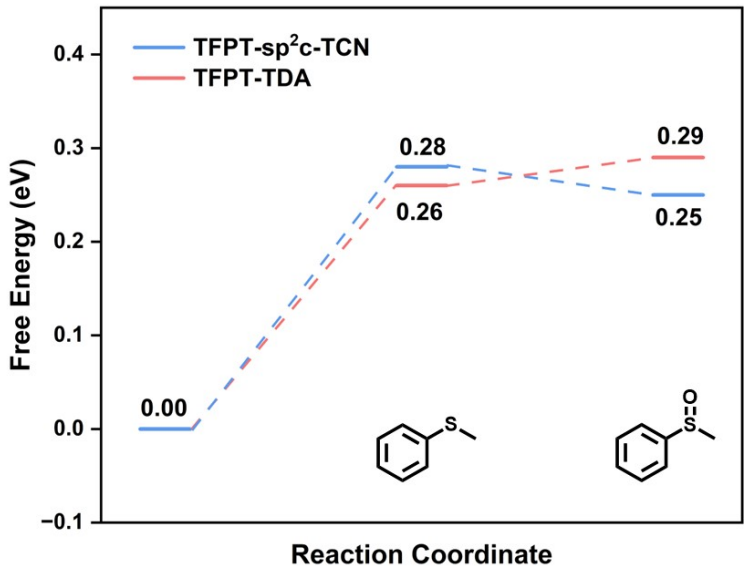

Fig. S10. Free energy calculation of COF to thioanisole to methyl phenyl sulfoxide

Table S1. Comparison of photocatalytic activity of the knot and linkers for the selective oxidation of thioanisole.[a]

Entry	Photocatalyst	Conv. (%)[b]	Sel. (%)[b]
1	TFPT	0	--
2	TCN	0	--
3	TDA	0	--

[a]Reaction conditions: photocatalyst (5 mg), thioanisole (0.3 mmol), MeOH (1 mL), blue LED irradiation, O_2 (0.1 MPa), 40 min. [b]The conversion and selectivity were determined by GC−FID.

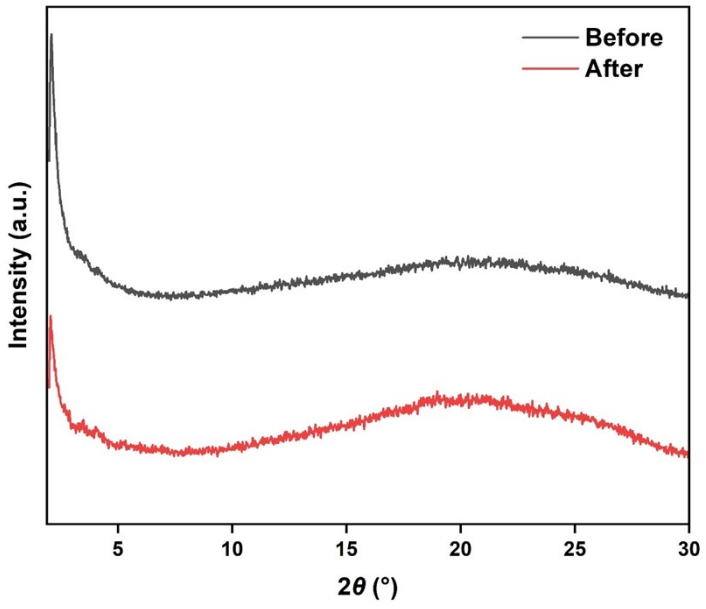

Fig. S11. PXRD patterns of TFPT-sp^{2}c-TCN before and after cycle experiments.

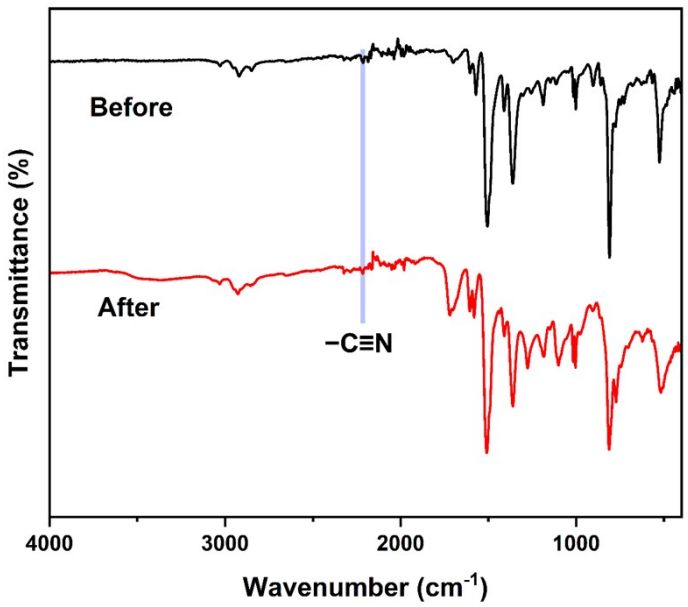

Fig. S12. FTIR spectra of TFPT-sp^{2}c-TCN before and after cycle experiments.

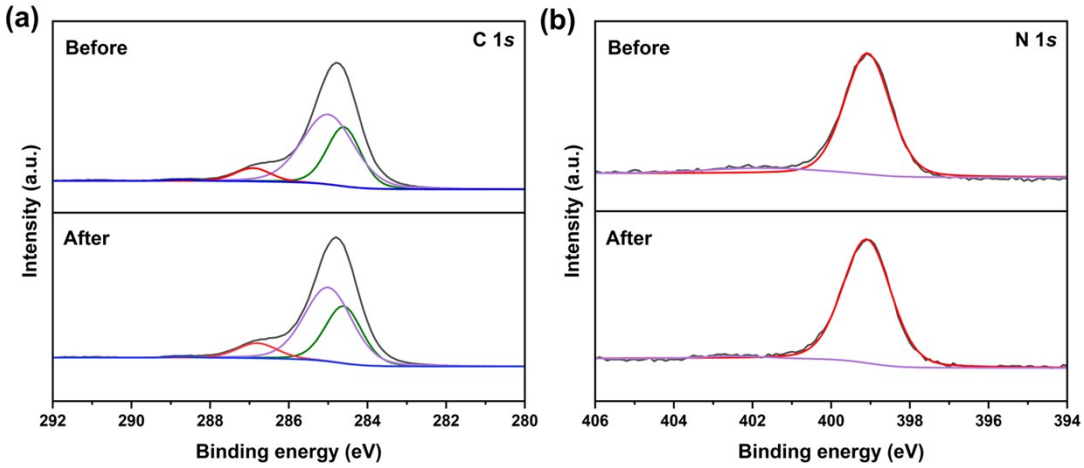

Fig. S13. C 1*s* and N 1*s* XPS spectra of TFPT-sp^{2}c-TCN before and after cycle experiments.

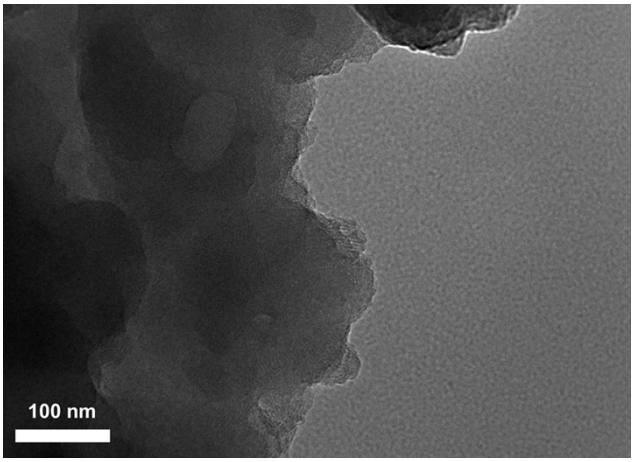

Fig. S14. TEM image of TFPT-sp^{2}c-TCN after cycle experiments.

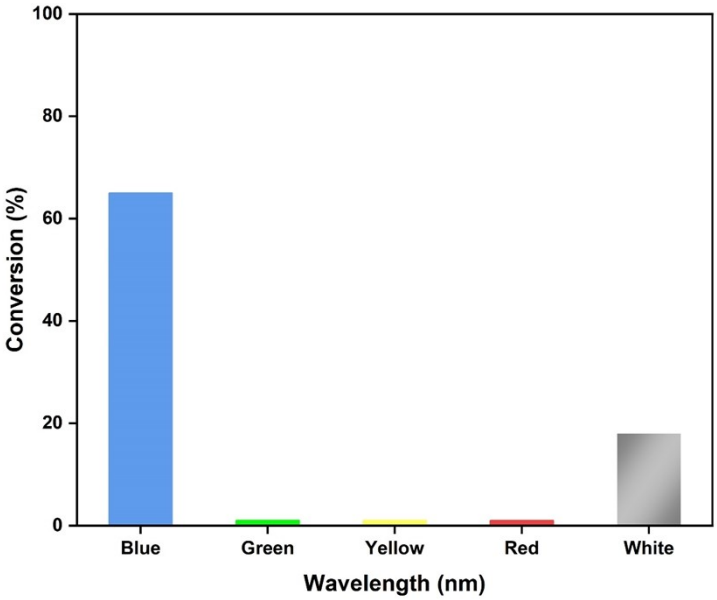

Fig. S15. The impact of different color LED irradiation on the selective oxidation of thioanisole over TFPT-sp^{2}c-TCN. Reaction conditions: TFPT-sp^{2}c-TCN (5 mg), thioanisole (0.3 mmol), MeOH (1 mL), LED irradiation, O_2 (0.1 MPa), 30 min.

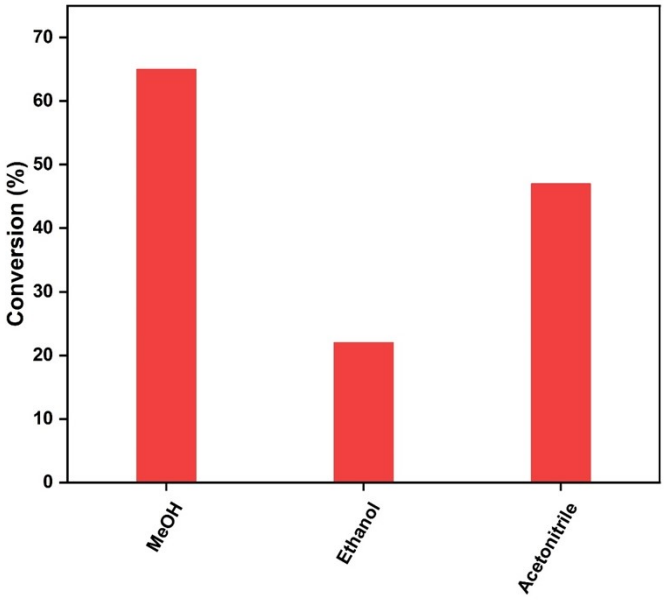

Fig. S16. The impact of different solvent on the selective photocatalytic oxidation of thioanisole over TFPT-sp^{2}c-TCN. Reaction conditions: TFPT-sp^{2}c-TCN (5 mg), thioanisole (0.3 mmol), solvent (1 mL), blue LED irradiation, O_2 (0.1 MPa), 30 min.

Table S2. Comparison of reported photocatalysts with TFPT-sp^{2}c-TCN for selective oxidation of thioanisole.

Photocatalysts	Conditions	t (h)	Conv. (%)	Sel. (%)	Ref.
TFPT-sp^{2}c-TCN (5 mg)	Sulfide (0.3 mmol), MeOH (1 mL), blue LEDs (460 ± 10 nm, 3W × 4), O_2 (0.1 MPa)	0.8	97	99	This work
CTF-PTZ (2 mg)	Sulfide (0.1 mmol), CD_3CN (1 mL), blue LEDs (3W × 4), air	2.0	99	94	[1]
AQ-COF (10 mg)	Sulfide (0.1 mmol), CH_3CN (2.0 mL), 300W Xe lamp (λ = 400–780 nm), O_2 (1 atm)	2	99	97	[2]
TP-PB COF (5 mg)	Sulfide (1.0 mmol), MeOH (2 mL), blue LEDs (460	12	93	99	[3]

	nm), O_2 (1 atm).				
UiO-66(Ce)-2A (20 mg)	Sulfide (0.1 mmol), MeOH (1.5 mL), 300 W Xe lamp (λ ≥ 400 nm), O_2 (0.1 MPa)	14	95.5	99	[4]
Ni_2P/BOB-OV (25 mg)	Sulfide (0.1 mmol), ARS (0.01 mmol), TEMPO (0.006 mmol), MeOH (5 mL), visible light (λ > 420 nm, 0.45 W/cm^2), O_2 atmosphere	3	97	99	[5]
Por-Phen-COF-N^+ (2.5 mg, porphyrin content 0.5 %)	Sulfide (0.3 mmol), CD_3OD (2 mL), Xe lamp (cut 420 nm), air	0.75	99	98	[6]
DClB-BTDF/g-C_3N_4 (10 mg)	Sulfide (2 mmol), 5 mL of CH_3CN/H_2O, blue LEDs (3 W ×4), O_2 (1 atm)	3.5	98	99	[7]

GC−FID results for Table 1.

Table 1, entry 1.

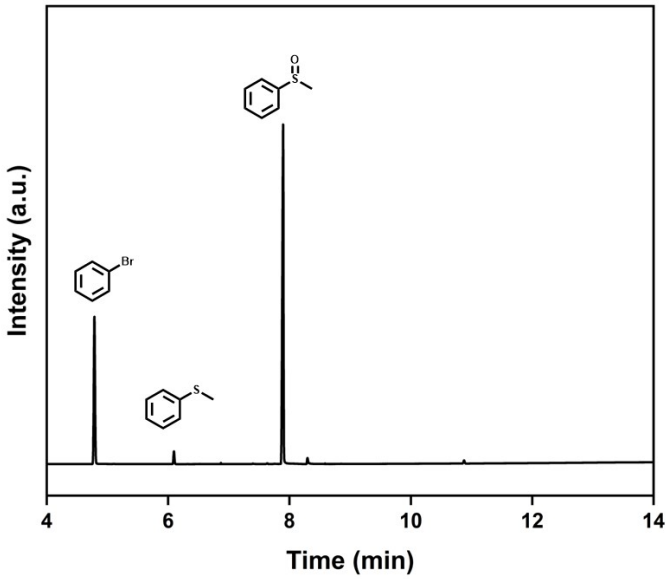

Table 1, entry 2.

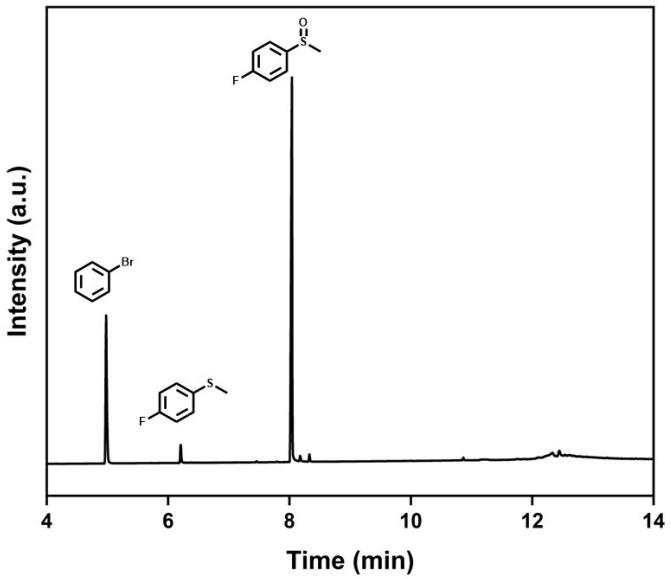

Table 1, entry 3.

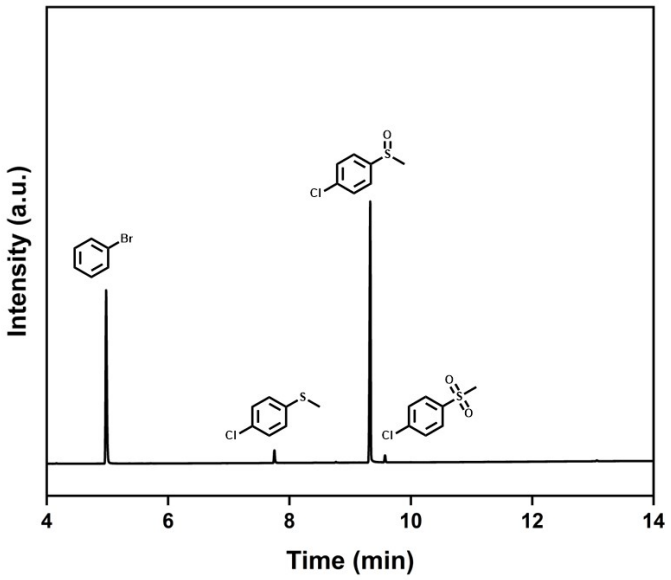

Table 1, entry 4.

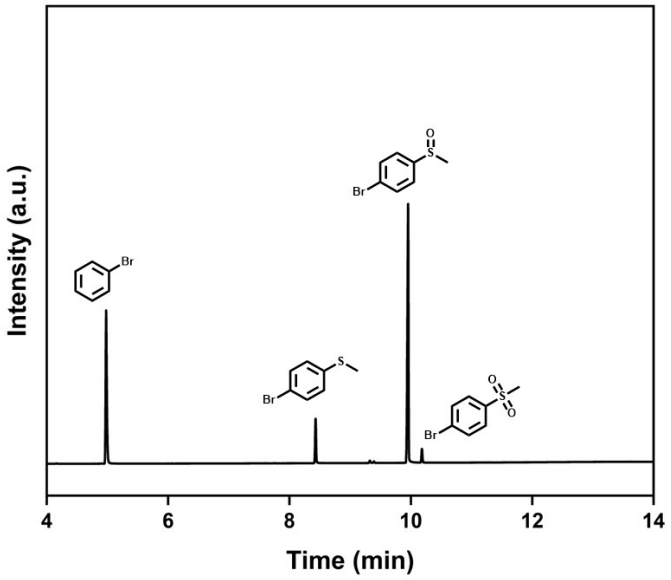

Table 1, entry 5.

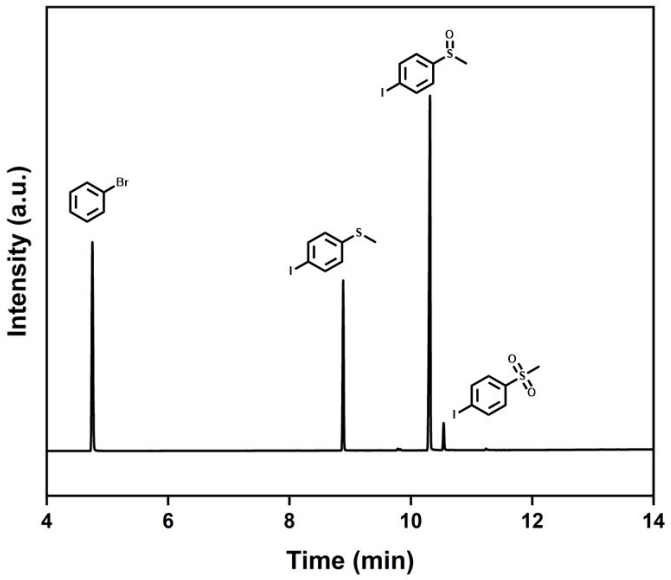

Table 1, entry 6.

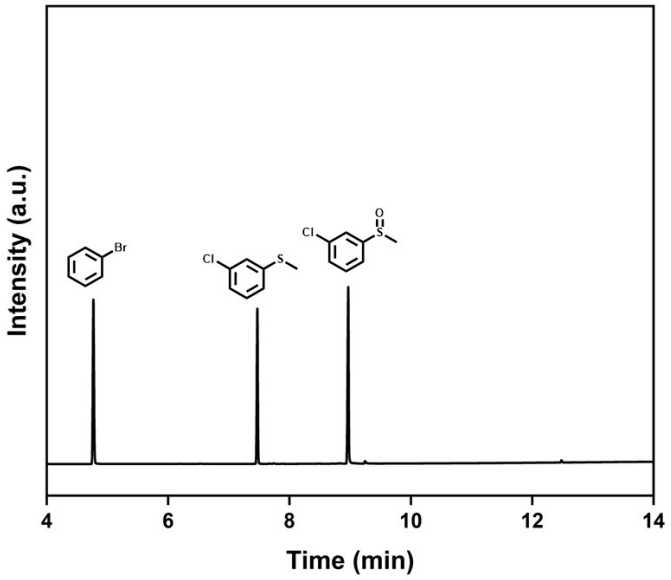

Table 1, entry 7.

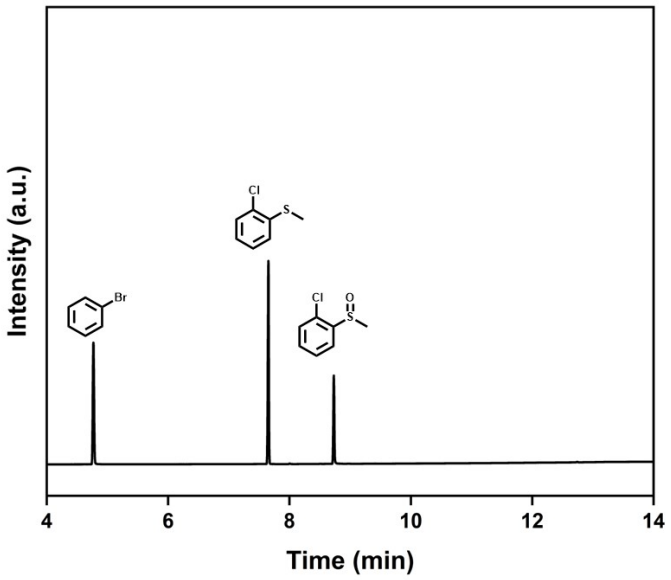

Table 1, entry 8.

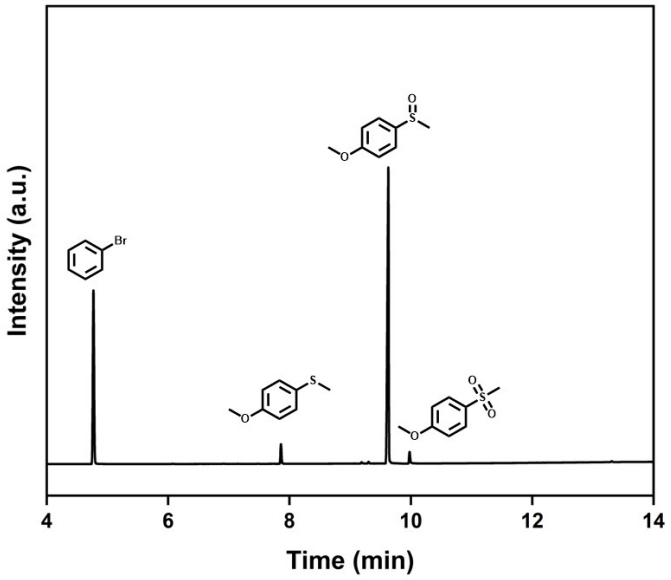

Table 1, entry 9.

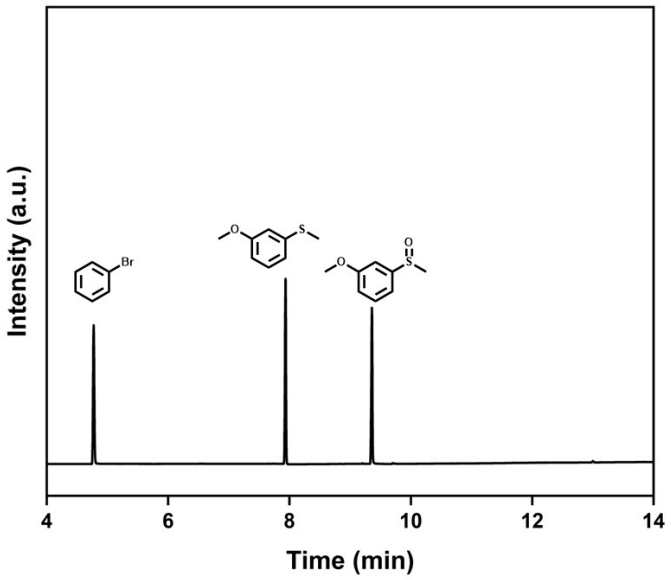

Table 1, entry 10.

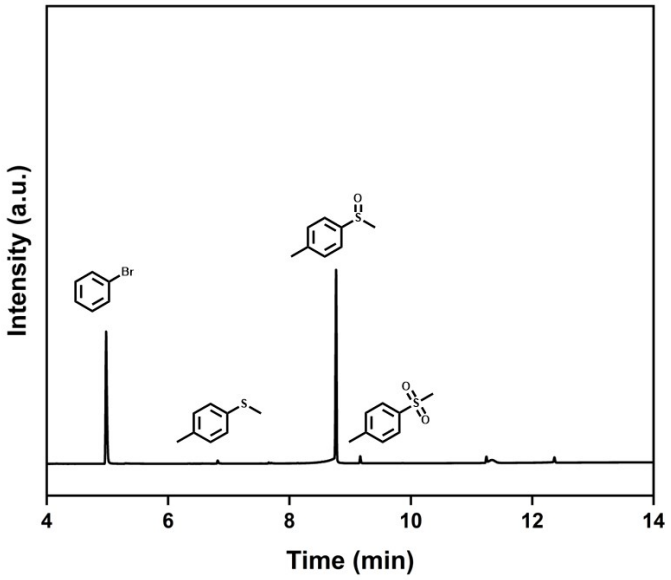

Table 1, entry 11.

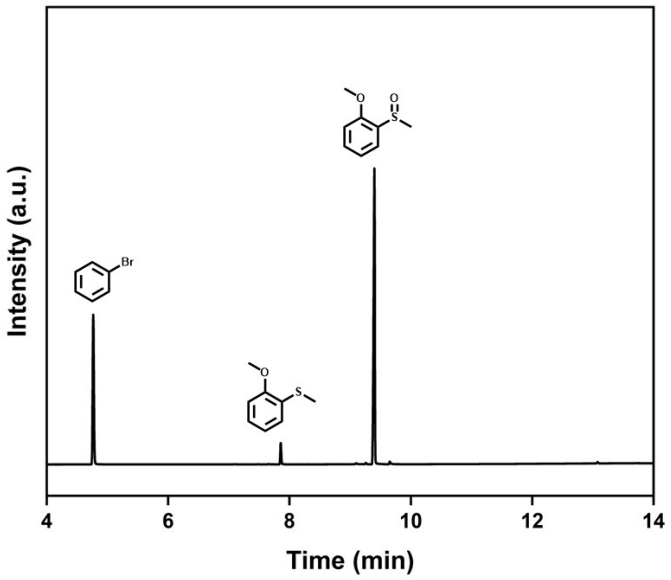

Table 1, entry 12.

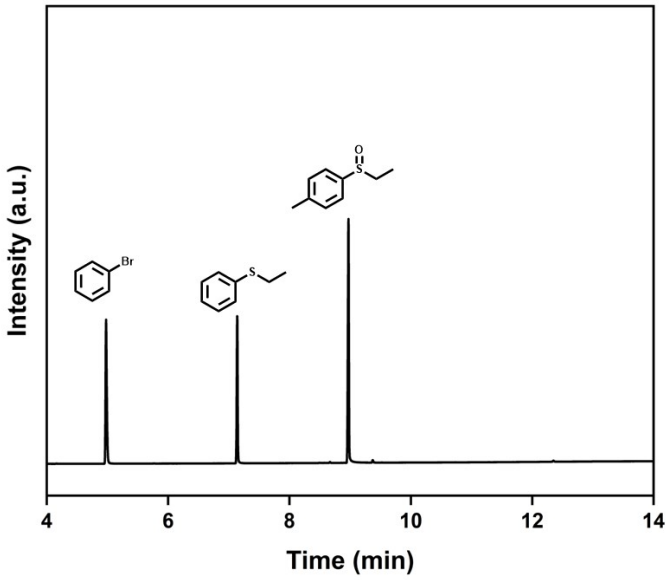

Table 1, entry 13.

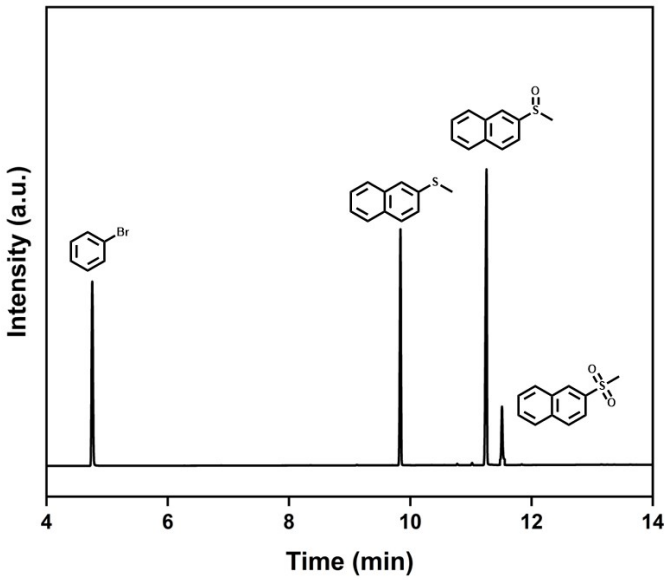

Table 1, entry 14.

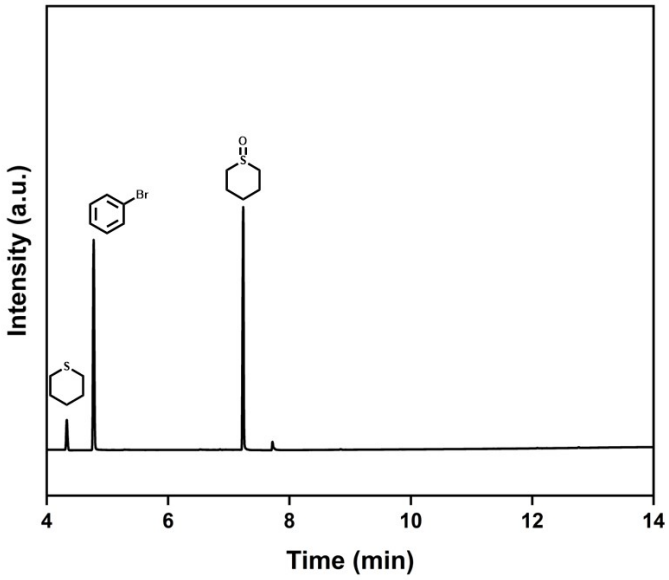

Table 1, entry 15.

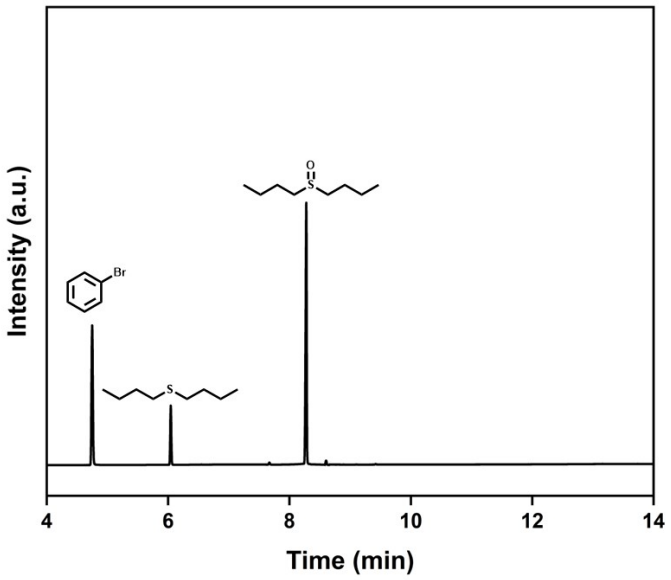

Leaching test.

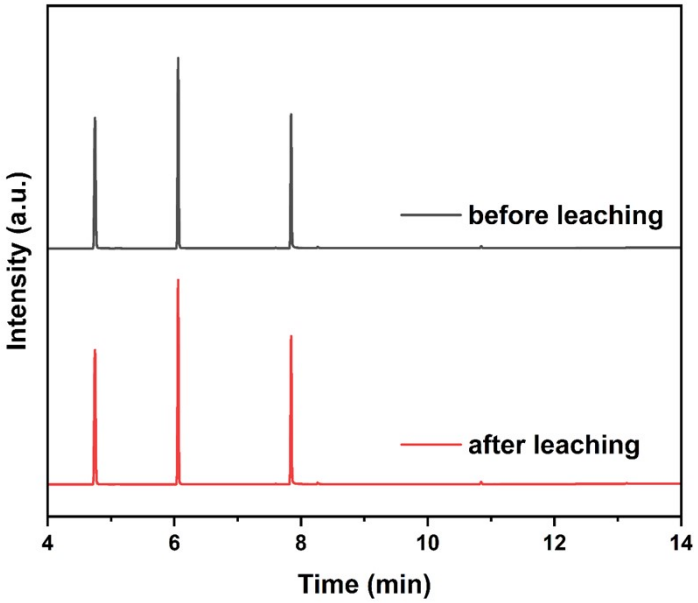

Reference

1. B. Wu, Y. Liu, Y. X. Zhang, L. Fan, Q. Y. Li, Z. Y. Yu, X. S. Zhao, Y. C. Zheng and X. J. Wang, *J. Mater. Chem. A*, 2022, **10**, 12489-12496.
2. F. Tao, W. W. Zhou, Z. Y. Li, X. K. Jiang, L. K. Wang, Z. P. Yu, J. Zhang and H. P. Zhou, *ACS Mater. Lett.*, 2024, **6**, 1120-1129.
3. Y. N. Du, Z. H. Wu, Y. J. Wang, J. Yang, H. Q. You, Y. X. Kong, H. Wu, Y. Wang, C. Cheng, S. Li and C. S. Zhao, *Small*, 2025, e12201.
4. C. Liu, Y. Z. Shi, Q. Chen, B. H. Ye, J. H. Bi, J. C. Yu and L. Wu, *Rare Met.*, 2025, **44**, 2462-2473.
5. W. J. Yang, K. L. Sun, J. Wan, Y. A. Ma, Y. Wang, L. Liu, B. C. Zhu and F. Fu, *Chem. Eng. J.*, 2023, **452**.
6. H. T. Lei, C. Y. Zhu, L. Lin, X. Y. Han, Y. Y. Ding, J. Song, Y. Y. Tian and G. S. Zhu, *Appl. Catal., B*, 2025, **361**.
7. C. Chu, Y. C. Qin, C. L. Ni, N. N. Wu and J. P. Zou, *Appl. Catal., B*, 2024, **341**, 123321.